

Observation of the Intraexciton Autler-Townes Effect in GaAs/AlGaAs Semiconductor Quantum Wells

Martin Wagner,¹ Harald Schneider,¹ Dominik Stehr,¹ Stephan Winnerl,¹ Aaron M. Andrews,² Stephan Schartner,² Gottfried Strasser,² and Manfred Helm¹

¹*Institute of Ion Beam Physics and Materials Research, Forschungszentrum Dresden-Rossendorf,
P.O. Box 510119, 01314 Dresden, Germany*

²*Micro- and Nanostructure Center, TU Wien, Floragasse 7, 1040 Vienna, Austria*

(Received 11 May 2010; published 12 October 2010)

The near-infrared transmission of a semiconductor multiple quantum well is probed under intense terahertz illumination. We observe clear evidence of the intraexcitonic Autler-Townes effect when the terahertz beam is tuned near the $1s$ - $2p$ transition of the heavy-hole exciton. The strongly coupled effective two-level system has been driven with terahertz field strengths of up to 10 kV/cm resulting in a Rabi energy of ≈ 0.6 times the transition energy. The induced near-infrared spectral changes at low intensities are qualitatively explained using a basic two-level model.

DOI: 10.1103/PhysRevLett.105.167401

PACS numbers: 78.67.De, 42.50.Hz, 73.21.Fg, 78.40.Fy

A fundamental problem in light-matter interaction is the coupling of an intense, monochromatic electromagnetic wave with a quantum mechanical two-level system. Many aspects of this scenario have been thoroughly investigated with atomic systems in connection with a third energy level, for instance, electromagnetic induced transparency (EIT) [1], lasing without inversion [2], and the Autler-Townes (or ac Stark) effect. The latter manifests itself in dressed light-matter states leading to a line splitting in a resonantly driven system [3,4]. Clear data on solid state systems, in particular, semiconductors, are more scarce, a reason being the short coherence times and the broad linewidths in these latter systems. A number of reports over the past decade have presented observations of various quantum optical phenomena in semiconductors, such as Rabi oscillations, the time-domain equivalent of the Autler-Townes effect, between donor states [5], interband transitions in quantum dots [6], intersubband transitions in quantum wells (QWs) [7], and intraexcitonic transitions in the midinfrared [8]. In the frequency domain, EIT [9,10] and gain without inversion [11] have been investigated as well as the Autler-Townes effect [12,13], but all in relation to QW intersubband transitions. Recently the latter phenomenon was also studied in quantum dots dressed by an interband excitation [14], and even in macroscopic Josephson junction based qubits [15,16], with both structures exhibiting small linewidths.

Particularly interesting systems are excitons in semiconductors, representing essentially the hydrogen problem energetically scaled down by a factor of 1000. Here we report the observation of the Autler-Townes effect of the intraexcitonic $1s$ - $2p$ absorption in semiconductor QWs. Since the $1s$ - $2p$ energy lies in the 10 meV (or THz) range, we can easily reach a regime where the dipole interaction energy and the ponderomotive energy approach the same order as the transition energy, a highly nonperturbative

regime requiring much higher intensities in atomic systems or for band gap transitions [17,18].

As a simplified description, we consider a monochromatic wave coupled to a two-level system, where the states get “dressed” by the light field, leading to (e.g., [19])

$$\hbar\omega_{1'} = \hbar\omega_1 - \hbar\Omega' \quad \text{and} \quad \hbar\omega_{2'} = \hbar\omega_2 + \hbar\Omega', \quad (1)$$

with $\Omega' = \frac{1}{2}\Delta \pm \frac{1}{2}\sqrt{\Delta^2 + \Omega^2}$ in the rotating-wave approximation (RWA), which requires $\Omega \ll \omega$. Here $\Delta = \omega - \omega_{21}$ is the detuning from the resonance frequency ω_{21} , and $\Omega = |\mu_{21}E|/\hbar$ denotes the Rabi frequency with the dipole matrix element μ_{21} and the electric field amplitude E . On resonance the original states split into doublets of energy $\hbar\omega_{1,2} \pm \hbar\Omega/2$, as sketched in Fig. 1(a).

Here we probe the near-infrared (NIR) transmission of an undoped GaAs/AlGaAs multiple quantum well (MQW) around the heavy-hole (HH) exciton while modulated via intense, in-plane polarized THz light. In-plane polarized THz light couples effectively to the $1s$ - $2p$ excitonic transition, as has been exploited in sideband generation [20,21], for the dynamical Franz-Keldysh effect [22], and for a determination of the dephasing time of the $1s$ - $2p$ transition [23]. Tuning the narrow band THz pump near the $1s$ - $2p$ resonance we observe clear signatures of a strongly coupled two-level system, i.e., an anticrossing of the dressed states depending on the THz photon energy and an intensity dependent Rabi splitting on resonance. Our investigations thus represent the first unambiguous observation of an intraexcitonic Autler-Townes effect.

The hydrogen-atom like $1s$ and $2p$ levels of the quantum well heavy-hole exciton are sketched in Fig. 1(b). Unlike the optically “bright” $1s$ and $2s$ states, the “dark” $2p$ state cannot be accessed in NIR transmission experiments because of quantum mechanical selection rules; however, it lies very close to the $2s$ state. Using optical-pump

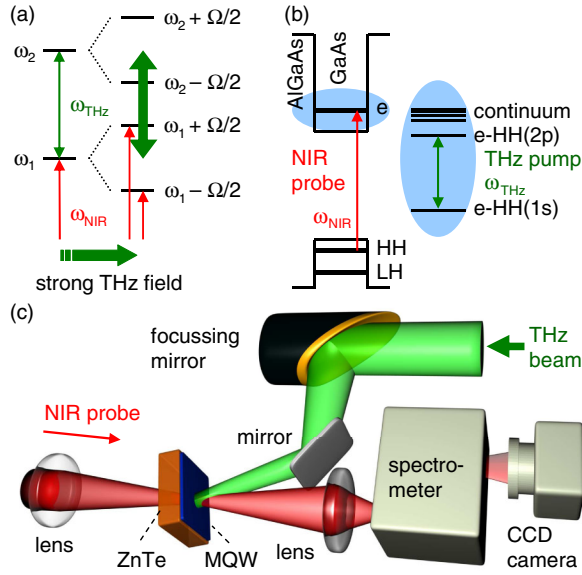


FIG. 1 (color online). (a) Autler-Townes splitting on resonance ($\omega_{\text{THz}} = \omega_{21}$) where the original states split by the Rabi frequency Ω . (b) Energy band diagram of a GaAs/AlGaAs quantum well with the electron (e) and heavy-hole (HH) and light-hole (LH) states. The THz pump beam is tuned to the $1s$ - $2p$ transition of the e -HH exciton. (c) Experimental geometry.

THz-time-domain spectroscopy [24], the $1s$ - $2p$ transition energy in our sample was determined to lie at $\hbar\omega_{21} \approx 9$ meV with a linewidth of 3 meV (FWHM).

Figure 1(c) displays the experimental setup. Broadband NIR light from a 12-fs Ti:sapphire laser (Femtolasers: Femtsource Scientific sPro) is focused at an angle of $\approx 15^\circ$ to the surface normal on the MQW film consisting of 60 periods of 8.2-nm thick GaAs quantum wells, separated by 19.6-nm thick barriers of $\text{Al}_{0.34}\text{Ga}_{0.66}\text{As}$. The substrate has been removed by wet etching, and the film of size 4×4 mm² was glued to a NIR transparent $\langle 100 \rangle$ -oriented ZnTe substrate. The transmitted light is analyzed by a grating spectrometer and a charge-coupled device camera. Strong THz light from the free-electron laser (FEL) FELBE of the Forschungszentrum Dresden-Rossendorf is focused and overlapped with the NIR probe spot at normal incidence on the sample. The NIR laser is synchronized and its repetition rate is reduced to 13 MHz, the same as of the FEL. The timing jitter between NIR and FEL pulses can be estimated to 1–2 ps, much shorter than the typical FEL pulse duration of 20–35 ps (FWHM). Their temporal overlap is adjusted via a rf phase shifter. The NIR probe light is attenuated to a peak intensity below 100 W/cm² in order not to modify the sample's absorption spectrum. The sample is kept in a liquid He flow cryostat at low temperature (near 10 K). Even at the highest presented THz peak intensities, the lattice temperature stays below 15 K, as determined by the small spectral shift (< 0.3 meV) of the main exciton line when the NIR probe pulse is delayed by 300 ps with respect to the FEL pulse. Such spectral shifts

due to a FEL induced lattice heating are already corrected for in the following spectra. In the experiment transmission spectra of the sample are recorded and normalized by the ZnTe substrate transmission before the absorption is calculated as the negative logarithm thereof.

In Fig. 2 absorption spectra are displayed for different time delays (in equidistant intervals of ≈ 2.7 ps) between the NIR probe and the FEL pump pulses with the THz photon energy at $\hbar\omega_{\text{THz}} = 10.5$ meV close to the $1s$ - $2p$ resonance. Probing 32 ps before the FEL pulse arrives (red bottom curve) reveals an unperturbed spectrum where the relevant states are indicated. Shifting the NIR probe pulse closer in time to the center of the FEL pulse drastically modifies the sample's absorption with a strong decrease at the e -HH($1s$) state and a minor decrease at the e -LH($1s$) state. But most strikingly the e -HH($1s$) exciton line splits, as is discussed in detail in the following paragraphs. Comparing the spectra with those obtained at the temporal overlap for different THz average powers, one can deduce a FEL pulse envelope with a nearly bandwidth-limited pulse width of ≈ 27 ps (FWHM), as shown on the right-hand side in the contour plot. We find that the absorption change occurs adiabatically on a time scale of several picoseconds, limited by the FEL pulse width and promising ultrafast optical switching or modulation.

Since the Autler-Townes effect manifests itself by a unique dependency on THz peak intensity and photon energy, we vary these parameters at the temporal overlap between pump and probe pulses, as shown in Fig. 3. For THz photon energies below the $1s$ - $2p$ resonance

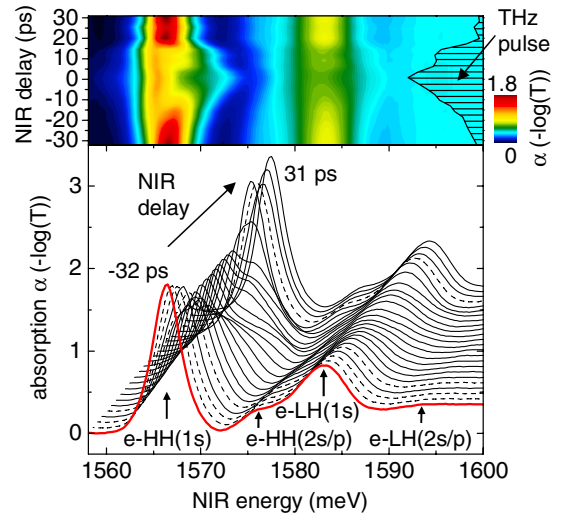


FIG. 2 (color online). Absorption at 10 K for different time delays between NIR probe and FEL pump pulses at a THz photon energy of 10.5 meV and a THz peak intensity of 500 kW/cm². The traces in the waterfall plot (bottom) are equally spaced in time. A few traces are interpolated between adjacent ones (dashed lines). Absorption peaks are labeled (lower red line). Above, the corresponding contour plot is shown. The right-hand inset displays the THz pulse intensity envelope.

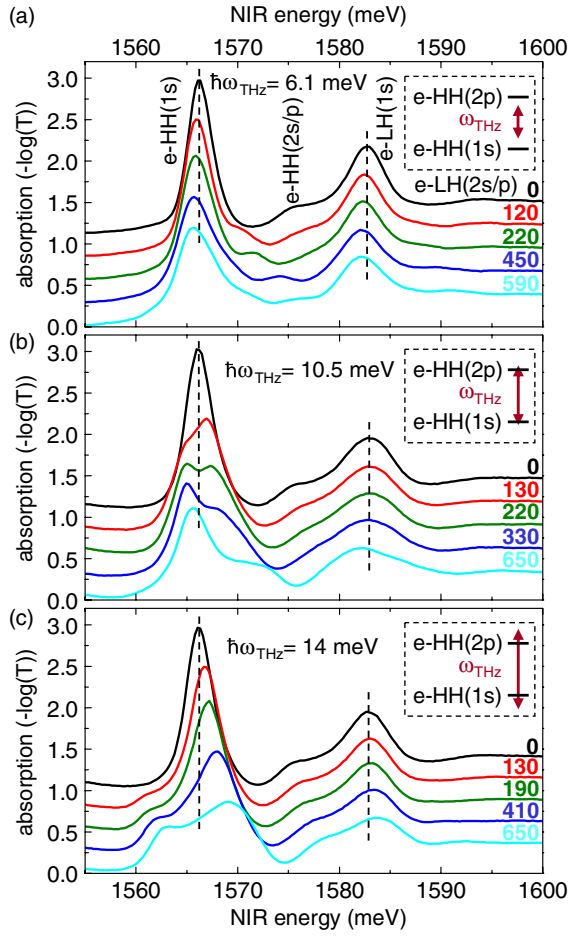


FIG. 3 (color online). Absorption spectra for different THz photon energies. Photon energies are tuned (a) below, (b) near, and (c) above resonance, as sketched in the insets. The low-temperature (10 K) spectra are vertically offset and labeled by THz peak intensities (in kW/cm^2). Vertical dashed lines mark the undriven $e\text{-HH}(1s)$ and $e\text{-LH}(1s)$ exciton resonances. Note that the given absolute THz peak intensities are estimated to be accurate within $\pm 30\%$ for different THz photon energies, whereas at the same photon energy relative intensities are accurate to $\pm 10\%$.

[$\hbar\omega_{\text{THz}} = 6.1$ meV in Fig. 3(a)], we clearly notice a small additional absorption peak evolving at 1570 meV and shifting to higher NIR energies with increasing THz peak intensity, while the main $e\text{-HH}(1s)$ peak slightly shifts towards lower energies. Its broadening could be explained by a beginning field ionization of the excitons, as known for strong in-plane dc electric fields [25]. Near resonance [$\hbar\omega_{\text{THz}} = 10.5$ meV, Fig. 3(b)] we observe a distinct splitting of the $e\text{-HH}(1s)$ absorption line. Note that the largest peak separation of 6 meV at $650 \text{ kW}/\text{cm}^2$ represents a significant fraction of the THz photon energy and the $1s\text{-}2p$ transition energy, a regime far beyond the RWA. An interesting but unexplained effect is the reversal of the relative absorption strengths of the dressed states with increasing pump intensity; i.e., consistent with a THz photon energy $\hbar\omega_{\text{THz}} > \hbar\omega_{21}$ the less absorptive dressed

state lies on the low-energy side for $130 \text{ kW}/\text{cm}^2$, while it is found on the high-energy side above $330 \text{ kW}/\text{cm}^2$, characteristic for $\hbar\omega_{\text{THz}} < \hbar\omega_{21}$. In between we find a symmetric splitting at $220 \text{ kW}/\text{cm}^2$ implying $\hbar\omega_{\text{THz}} \approx \hbar\omega_{21}$. This reversal indicating a dynamic blueshift of the $1s\text{-}2p$ resonance is also present in the delay dependent absorption spectra in Fig. 2 for the time steps of 14.5–17.2 ps, and $-10.2\text{--}15.7$ ps, respectively. Above resonance [$\hbar\omega_{\text{THz}} = 14$ meV, Fig. 3(c)] a FEL induced peak appears below the $e\text{-HH}(1s)$ peak that is now blueshifted with increasing THz peak intensity. Compared to the unperturbed case, we observe a 20-fold increase in transmission at the $e\text{-HH}(1s)$ exciton for $650 \text{ kW}/\text{cm}^2$, i.e., a large transmission change suitable for an optical modulator. We note that similar but much weaker signatures are seen at the $e\text{-LH}(1s)$ state, which will not be discussed further here.

Figure 4(a) displays the measured peak positions obtained from a two-line fit around the undriven $e\text{-HH}(1s)$ exciton (marked as dashed horizontal line) for different THz photon energies at $\approx 130 \text{ kW}/\text{cm}^2$. These data points agree reasonably well with the anticrossing behavior (solid red lines) predicted by the simple two-level model according to Eq. (1) where the resonance energy $\hbar\omega_{21} = 9$ meV enters and the Rabi frequency was fitted to $\Omega = 0.25\omega_{21}$. Away from resonance the peak separation is largest and the absorption strength (indicated by a gray scale) is most pronounced for the dressed state closest to the undriven $e\text{-HH}(1s)$ exciton. Close to resonance the separation is smallest and the absorption strength is shared equally.

On resonance the two-level model predicts a splitting proportional to the Rabi energy and hence to the THz field, which is confirmed in Fig. 4(b) for $\hbar\omega_{\text{THz}} = 10.5$ meV. The linearity is preserved up to a THz peak intensity of

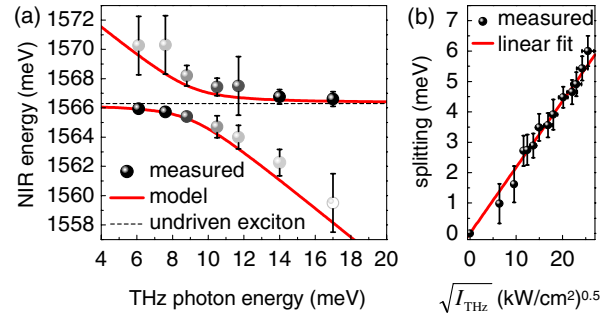


FIG. 4 (color online). Experiment-model comparison. (a) Measured peak positions for different THz photon energies at a THz peak intensity $I_{\text{THz}} \approx 130 \text{ kW}/\text{cm}^2$. The absorption strength is indicated by a gray scale (more absorption for dark points). Error bars denote deviations based on several measurements and the uncertainty in the THz peak intensity. Solid red lines represent the calculation according to Eq. (1) (see text). (b) Separation between the split peaks for $\hbar\omega_{\text{THz}} = 10.5$ meV near resonance. Vertical error bars are related to the error in the fitted peak positions, the horizontal ones to the uncertainty in the THz peak intensity.

650 kW/cm² with a Rabi energy $\Omega \approx 0.6\omega_{21}$, well beyond the RWA of our model. Assuming an intensity to field relation $I_{\text{THz}} = \frac{1}{2}\epsilon_0 c_0 n E_{\text{THz}}^2$ from a plane wave with a refractive index $n \approx 3.61$ [26], we estimate a THz field strength of $E_{\text{THz}} \approx 10$ kV/cm within the sample (30% reflection losses). Apparently, the simple two-level model holds true up to this moderate field strength. Note that the ponderomotive energy $U_p = e^2 E_{\text{THz}}^2 / (4m^* \omega_{\text{THz}}^2)$ [22] as the mean oscillatory energy of an electron in the light field is 3 meV and thus of the same order as the Rabi energy, the exciton transition energy, and the ionization energy E_i , an extremely nonperturbative regime with a Keldysh parameter $\gamma = \sqrt{E_i / (2U_p)}$ near unity. We emphasize that despite large linewidths it is possible to study this complex regime in a quantum well exciton exposed to intense THz pulses, whereas it is difficult to address this region experimentally in atomic spectroscopy with its much larger level separations.

Differences from a simple two-level system are expected for our configuration since (i) the system comprises many excitonic levels and continuum states interacting with the THz radiation, (ii) the RWA breaks down, and this happens earlier for lower THz photon energies, (iii) exciton field ionization starts [25], and (iv) the dynamical Franz-Keldysh effect can occur in our experimental geometry [22]. What also cannot be explained within the two-level model is the peak reversal as a function of THz intensity [Fig. 3(b)]. Consequently, a more precise theoretical treatment, based on the full semiconductor Bloch equations [27,28], seems more applicable.

However, the measured Autler-Townes splitting can be compared quantitatively with the Rabi energy estimated from the dipole matrix element. Since the exciton behaves similar to a hydrogen atom, we evaluate the hydrogen $1s$ - $2p$ transition matrix element $\mu_{21} = 0.745ea_0^*$ [19] (with charge e). The exciton wave function is compressed in the quantum well growth direction. Hence the effective Bohr radius $a_0^* = 0.25(\alpha - 1)^2 m_e \epsilon a_0 / \mu^*$ depends on the fractional dimension α [29]. With $\epsilon = 13$, Bohr radius a_0 , reduced exciton mass $\mu^* = 0.059m_e$, and $\alpha \approx 2.43$ for our system [30], we find $\mu_{21} \approx 44$ eÅ and a Rabi energy of 2.4 meV for a THz field strength of $E_{\text{THz}} \approx 5.4$ kV/cm, corresponding to a peak intensity of 200 kW/cm². Experimentally we observe an Autler-Townes splitting of 3 meV, which is in good agreement with the calculated value from simplified considerations.

In conclusion, we have reported a remarkably large absorption change and induced line splitting in the near-infrared spectral region around the e -HH($1s$) exciton when modulated at THz frequencies in a normal-incidence geometry at low temperature. The signatures are observed on a time scale of several picoseconds and are interpreted as

an intraexcitonic ac Stark effect originating from the dressing of the excitonic $1s$ and $2p$ states by the THz field. The system has been driven up to a THz field strength of ≈ 10 kV/cm with a Rabi energy of ≈ 0.6 times the transition energy, a region well beyond the rotating-wave approximation and with a Keldysh parameter near unity. Moreover, the appearance of dressed states in this regime indicates a remarkably weak coupling of the $2p$ state to the continuum. Finally, with a 20-fold transmission change during picosecond pulses our approach provides a simple scheme for an ultrafast, normal-incidence optical modulator.

We thank P. Michel and his FELBE team for their dedicated support, as well as W. Seidel, F. Peter, and J. Kono for friendly cooperation and fruitful discussions. The Vienna group is supported by the Austrian FWF (SFB IR-ON).

-
- [1] K.-J. Boller, A. Imamoglu, and S.E. Harris, *Phys. Rev. Lett.* **66**, 2593 (1991).
 - [2] A. S. Zibrov *et al.*, *Phys. Rev. Lett.* **75**, 1499 (1995).
 - [3] S. H. Autler and C. H. Townes, *Phys. Rev.* **100**, 703 (1955).
 - [4] J. S. Bakos, *Phys. Rep.* **31**, 209 (1977).
 - [5] B. E. Cole *et al.*, *Nature (London)* **410**, 60 (2001).
 - [6] A. Zrenner *et al.*, *Nature (London)* **418**, 612 (2002).
 - [7] C. W. Luo *et al.*, *Phys. Rev. Lett.* **92**, 047402 (2004).
 - [8] S. Leinss *et al.*, *Phys. Rev. Lett.* **101**, 246401 (2008).
 - [9] G. B. Serapiglia *et al.*, *Phys. Rev. Lett.* **84**, 1019 (2000).
 - [10] M. C. Phillips *et al.*, *Phys. Rev. Lett.* **91**, 183602 (2003).
 - [11] M. D. Frogley *et al.*, *Nature Mater.* **5**, 175 (2006).
 - [12] J. F. Dynes *et al.*, *Phys. Rev. Lett.* **94**, 157403 (2005).
 - [13] S. G. Carter *et al.*, *Science* **310**, 651 (2005).
 - [14] X. Xu *et al.*, *Science* **317**, 929 (2007).
 - [15] M. Baur *et al.*, *Phys. Rev. Lett.* **102**, 243602 (2009).
 - [16] M. A. Sillanpää *et al.*, *Phys. Rev. Lett.* **103**, 193601 (2009).
 - [17] O. D. Mücke *et al.*, *Phys. Rev. Lett.* **87**, 057401 (2001).
 - [18] Q. T. Vu *et al.*, *Phys. Rev. Lett.* **92**, 217403 (2004).
 - [19] P. W. Milonni and J. H. Eberly, *Lasers* (John Wiley & Sons, New York, 1988).
 - [20] J. Kono *et al.*, *Phys. Rev. Lett.* **79**, 1758 (1997).
 - [21] M. Wagner *et al.*, *Appl. Phys. Lett.* **94**, 241105 (2009).
 - [22] K. B. Nordstrom *et al.*, *Phys. Rev. Lett.* **81**, 457 (1998).
 - [23] A. D. Jameson *et al.*, *Appl. Phys. Lett.* **95**, 201107 (2009).
 - [24] R. A. Kaindl *et al.*, *Nature (London)* **423**, 734 (2003).
 - [25] D. A. B. Miller *et al.*, *Phys. Rev. B* **32**, 1043 (1985).
 - [26] J. N. Heyman, R. Kersting, and K. Unterrainer, *Appl. Phys. Lett.* **72**, 644 (1998).
 - [27] M. Kira and S. W. Koch, *Prog. Quantum Electron.* **30**, 155 (2006).
 - [28] J. T. Steiner, M. Kira, and S. W. Koch, *Phys. Rev. B* **77**, 165308 (2008).
 - [29] X.-F. He, *Phys. Rev. B* **43**, 2063 (1991).
 - [30] H. Mathieu, P. Lefebvre, and P. Christol, *Phys. Rev. B* **46**, 4092 (1992).